Journal of Applied Polymer Science

Nanomechanical Properties of Poly(trimethylene malonate) and Poly(trimethylene itaconate) During Hydrolytic Degradation

Ersan Eyiler,[1] I.-W. Chu,[2] Mathew D. Rowe,[2] Keisha B. Walters[2]

[1]Department of Chemical Engineering, Cukurova University, Ceyhan, Adana 01950, Turkey

[2]Dave C. Swalm School of Chemical Engineering, Mississippi State University, Mississippi State, Mississippi 39762

Correspondence to: K. B. Walters (E-mail: kwalters@che.msstate.edu)

ABSTRACT: The aim of this work was to evaluate surface mechanical properties of two bioplastics, poly(trimethylene malonate) (PTM) and poly(trimethylene itaconate) (PTI), during hydrolytic degradation. Renewable resource-based PTM and PTI were synthesized from 1,3-propanediol (PDO), malonic acid (MA), and itaconic acid (IA) via melt polycondensation. The hydrolytic degradation was performed in deionized (DI) water (pH 5.4) at room temperature. Morphology and surface mechanical properties at the nanoscale were monitored by atomic force microscopy (AFM) using a quantitative nanomechanical property mapping mode as a function of degradation time. Differential scanning calorimetry (DSC) and thermogravimetric analysis (TGA) were used to show shifted phase transitions depending on the degradation. DSC studies showed hydrolytic degradation induced crystallinity for PTI. After degradation for one week, the degree of crystallinity had significantly increased, and the elastic modulus of PTI had decreased by 58%. PTM was found to be hygroscopic. © 2014 Wiley Periodicals, Inc. J. Appl. Polym. Sci. **2014**, *131*, 41069.

KEYWORDS: biopolymers and renewable polymers; degradation; differential scanning calorimetry (DSC); mechanical properties; polyesters

Received 14 October 2013; accepted 12 May 2014

DOI: 10.1002/app.41069

INTRODUCTION

Polymers are good substitutes for metal, paper, and glass since they demonstrate suitable energy savings, weight savings, and/or durability. Bioplastics are polymeric materials produced from biomass-derived monomers, and also often can be biologically and/or hydrolytically degradable. Polyhydroxyalkanoates, poly (lactic acid), poly(glycolic acid), polysaccharides, vegetable-derived polymers, and poly(orthester) are just a few examples of different bioplastic types/classes.[1–5] These plastics span a range of physicochemical properties, cost, and degradation rates, and have the potential to compete with petroleum-based plastics in terms of properties and cost.[6–11]

Biorefineries that produce multiple products, including higher-value chemicals as well as fuels and power, have become significant advancement toward reducing fossil fuel dependency. For this reason, in 2004, the U.S. Department of Energy (DOE) identified 12 building block chemicals derived from sugars that can serve as key feedstocks for future biorefineries due to their functionality, availability, toxicity, and possible derivatives.[12] These chemicals and their derivatives have the potential to be biomonomers used for production of bioplastics.

Using several monomers from the DOE 12 building blocks list, two bio-based copolymers, poly(trimethylene malonate) (PTM) and poly(trimethylene itaconate) (PTI), have been produced with ester bonds incorporated into the polymer backbone to facilitate hydrolytic and/or enzymatic degradation as described previously.[13] PTM was synthesized from 1,3-propane diol and malonic acid to produce a linear copolymer, and PTI was synthesized from 1,3-propane diol and itaconic acid to produce a branched and possibly cross-linked copolymer. For specialty applications, the hydrolytic behavior of these bioplastics needs to be evaluated with mechanical properties. In this article, we present a hydrolytic degradation study in deionized (DI) water, addressing this purpose. Weight change was monitored as a function of degradation time (10–10,000 min). More importantly, effects of hydrolytic degradation on the surface mechanical properties were examined by atomic force microscopy (AFM) at the nanoscale.

EXPERIMENTAL

Materials

Malonic acid (MA, 99%), itaconic acid (IA, 99%) and chloroform (98%) were used as received from VWR. 1,3-Propane diol (PDO, 98%), aluminum chloride (98%), and diethyl ether (>99%) were used as received from Sigma-Aldrich.

Poly(trimethylene malonate) (PTM) and poly(trimethylene itaconate) (PTI) were synthesized via melt polycondensation as

described previously.[13] In brief, polymerizations were performed in a 100-mL round bottom flask at 25 torr. For PTM and PTI, PDO and MA or PDO and IA, respectively, were fed at a 1:1 molar ratio using a 100:1 monomer to catalyst ($AlCl_3$) ratio. The flask was then immediately placed into an oil bath at 155°C, and the polymerizations were carried out for 4 h for PDO-MA and 16 h for PDO-IA. When the reactions were completed, excess monomer and catalyst were removed by dissolving the reaction product in chloroform. This chloroform solution was then poured into diethyl ether. The polymer precipitated out of solution and was removed by filtration using Whatman (grade 40) filter paper. The filtered polymer was then dried in a vacuum oven at 15 torr and 20°C for 24 h.

Hydrolytic Degradation

PTM was compression molded into a 12 cm × 12 cm × 0.159 cm sheet using a Carver 15 ton hydraulic press at 6.9 MPa and 30°C for 10 min. The sheet was cut into 1 cm × 0.318 cm × 0.318 cm coupons. PTI was ground by hand into a powder using a mortar and pestle until all particles could easily sift through 18 × 18 mesh stainless steel wire cloth.

For the PTM hydrolysis experiment, the samples were initially placed under vacuum at room temperature for 24 h to remove excess water. Vials were then prepared containing one compression molded PTM coupon along with 10 mL DI water (pH 5.4). One set of sample vials contained no liquid and was used as an "air" control, to take into account any changes due to nonhydrolytic aging. The sample vials were then sealed and placed into a 25°C water bath for 10, 100, 1000, or 10,000 min.

For each PTI sample, 0.75 g of PTI powder was placed into a 16 mL clear glass vial and 10 mL DI water were added. One set of PTI samples had no solution added as an "air" control. The sealed vials were placed into a 25°C water bath for 100, 1,000, or 10,000 min.

At each predesignated time, samples were removed from solution and gently blotted with a KimWipe®. They were then vacuum dried (25 torr) at room temperature for 24 h and then dry sample weights were recorded. All degradation samples were run in triplicate.

Gel Permeation Chromatography (GPC)

Gel permeation chromatography (GPC) data was collected with a Waters GPC with RI detector, 4E and 5E (polystyrene-dinvinylbenzene, 4.6 × 300 mm) Styragel® columns, Optima THF as the effluent at 0.3 mL/min, and a 10-point polystyrene calibration.

Thermogravimetric Analysis (TGA)

A TA Instruments Q-600 simultaneous DSC/TGA (SDT) instrument with the TA Universal Analysis 2000 software (v4.7A) was used to assess the thermal stability of the degraded PTM and PTI samples. The 5 mg samples were analyzed from room temperature to 600°C at a rate of 10°C/min under 50 mL/min of nitrogen purge.

Differential Scanning Calorimetry (DSC)

A TA Instruments Q-2000 modulated DSC (mDSC) with the TA Universal Analysis 2000 software (v4.7A) was used for thermal analysis of the degraded PTM and PTI samples. The 5 mg samples were heated from 40 to 270°C at a rate of 10°C/min under 50 mL/min of nitrogen purge. The cold crystallization temperature (T_{cc}), melting temperature (T_m), and melting enthalpy (ΔH_m) of the degraded PTI samples were determined from the exotherms, and the degree of crystallinity (X_m) was not calculated since the melting enthalpy for 100% crystalline PTI is unknown.

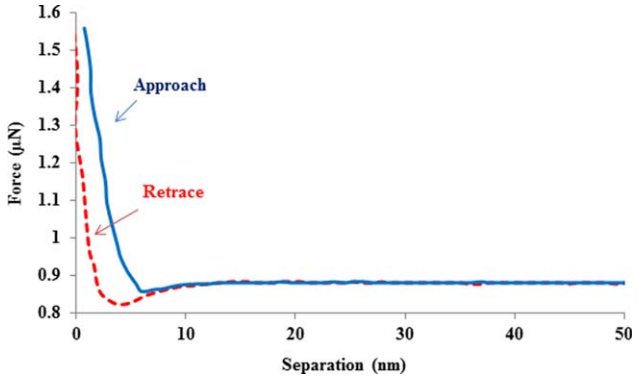

Figure 1. Force-separation curve to obtain the mechanical properties of the sample. [Color figure can be viewed in the online issue, which is available at wileyonlinelibrary.com.]

Atomic Force Microscopy (AFM)

In this study, a new AFM mode known as "PeakForce QNM" was used on a Dimension Icon AFM to map the mechanical properties of the bioplastic samples. By using PeakForce Tapping™, damage to the tip and sample can be minimized by directly controlling the forces applied to the tip and using forces lower than those generally used in tapping mode. This method also allows for better control of the maximum force (PeakForce) on the tip as it ensures that the tip-sample contact area is as small as possible.[14]

During the tapping, the AFM generates force curves for each pixel on the sample surface and converts them to the force-separation plots that give some of the major mechanical properties such as elastic modulus, adhesion, dissipation, and deformation. Figure 1 shows the force-separation curve during a single peak force tapping.

The Derjaguin-Muller-Toporov (DMT) model can be used to fit the retract curve in order to estimate the reduced modulus, E^*.[14] The DMT model uses Eqn. 1 with the relationship between modulus and forces given as

$$E^* = \frac{3}{4}(F - F_{adh})/\sqrt{R(d-d_0)^3} \quad (1)$$

where E^* is the reduced elastic modulus of the sample, R is the tip radius, $(F - F_{adh})$ is the difference between the relative forces of the tip and adhesion during the tapping, and $(d - d_0)$ is the sample deformation. Young's modulus of the sample (E_s) can be calculated directly from the reduced modulus by using the known Poisson's ratio of the sample

$$E^* = \left[\frac{1-v_s^2}{E_s} + \frac{1-v_{tip}^2}{E_{tip}}\right]^{-1} \quad (2)$$

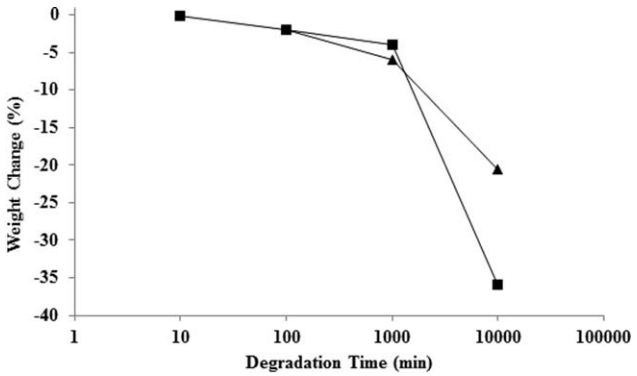

Figure 2. Weight loss of PTM (□) and PTI (Δ) in DI water as a function of degradation time.

where E_s is the Young's modulus of the sample, E_{tip} is the modulus of the tip, and v_s and v_{tip} are the Poisson's ratios of the sample and the tip, respectively. Here, the elastic modulus of the tip (E_{tip}) can be assumed infinite.[14]

First, the appropriate cantilever was selected based on the sample type and calibrated to measure its sensitivity, spring constant, and radius; a TAP525A probe with tip radius of 10 nm was used. All mechanical analyses of PTI as a function of the hydrolytic degradation were performed in air at ambient temperature. The PTI samples were attached onto the metal AFM pan using adhesive tape. The scanning rate was less than 1 Hz and 512 × 512 pixels were used for 5 × 5 μm scans. The peakforce set-point and the Poisson's ratio were set to 3.0 μN and 0.3, respectively. After the PeakForce Tapping™ was performed, the AFM images were analyzed with the NanoScope Analysis software (v1.40).

RESULTS AND DISCUSSION

Hydrolytic Degradation

A hydrolytic degradation study was performed on the bioplastics, PTM and PTI in DI water at room temperature. During the degradation, the diffusion of acidic monomers and oligomers into the solution caused the pH of the solution to become acidic (~pH 3.4). Weight change was monitored as a function of degradation time (10 × 10,000 min) to determine if degradation was occurring. Final weight loss varied from 20 to 37 wt % for PTM and from 7 to 21 wt % for PTI as a function of degradation time (Figure 2). The reaction mechanisms during acid-catalyzed ester hydrolysis can be seen in Figure 3 and require an excess of water to drive the reactions to completion.

Molecular weight (M_w) changes were examined for both PTM and PTI using GPC. PTM experienced significant decreases in M_w as a function of time, Table I. In the first 10 min, no significant decrease in M_w indicates that the low M_w material diffused out of PTM. If the low M_w PTM was diffusing out, the PDI should have decreased, which does occur. The solution become more acidic in the initial 10 min as low M_w material diffuses into the solution, and the acidic solution facilitates the acid catalyzed ester hydrolyses through the $A_{AC}2$ and $A_{AL}1$ mechanisms. By 100 min, there is a significant increase in PDI as the $A_{AC}2$ and $A_{AL}1$ mechanisms degrade ester bonds with a lack of degradation product diffusion out of the samples. At 1000 and 10,000 min, the M_w significantly decreases from ~2100 Da to 1600 Da and 1300 Da, respectively. The PDI decrease at 1000 and 10,000 min as diffusion is able to remove degradation products.

PTI exhibited significant degradation from 100 to 10,000 min as shown by the weight change before. PTI did initially have a bimodal Mw distribution (Table I). The higher M_w polymer was above 10,000 Da and will be referred to as HMw. The lower M_w polymer was below 10,000 Da and will be referred to as LMw. During the initial 100 min, LMw increased by ~100 Da when compared with the initial value. The increase in LMw is due to the diffusion of polymer into the solution, and this diffusion causes the pH of the solution to become more acidic. From 100 to 1000 min, the PDI appear to increase from ~1.7 to ~1.8. The increase in PDI with no change in M_w shows that degradation is occurring, and the degradation products have not diffused out of the polymer leading to an increase in PDI. From 1000 min to 10,000 min, the molecular weight decreased by 200 Da, and the PDI decreased from ~1.8 to ~1.7 as hydrolytic degradation occurs, and LMw material diffuse into the aqueous phase. In 1000 min, the high molecular weight material, HMw, decreased by time; however, PDI remained the same. After 1000 min, the HMw was not detected, and it is assumed that the HMw has degraded to a point at which it is indistinguishable from the lower M_w material.

Thermal Properties

The thermal behavior of the neat (nondegraded, 0 min) and degraded PTM and PTI samples were analyzed by DSC. The data are presented in Table II, and the heating thermograms are

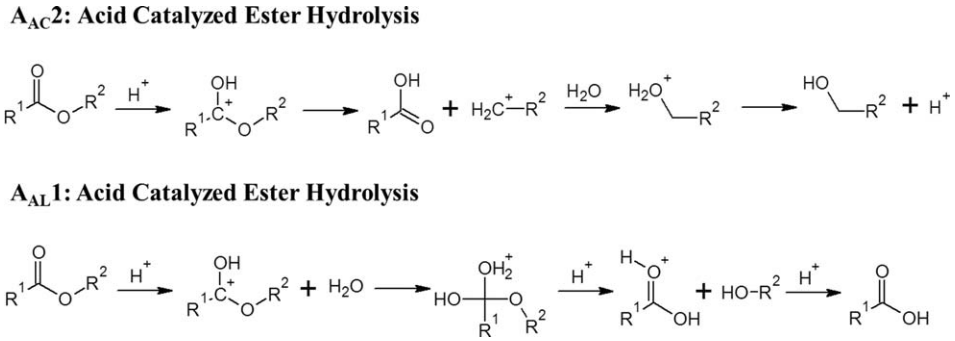

Figure 3. The $A_{AC}2$ and $A_{AL}1$ ester hydrolysis reaction mechanisms.

Table I. Molecular Weight Data of PTM and PTI Samples as a Function of Degradation Time

Polymer	Degradation Time (min)	HM_w (Da)	PDI	LM_w (Da)	PDI
PTM	0	62,950 ± 504	1.8 ± 0.2	1,791 ± 62	1.8 ± 0.0
	10	—	—	2,070 ± 86	1.6 ± 0.1
	100	—	—	2,053 ± 42	1.7 ± 0.0
	1,000	—	—	1,630 ± 27	1.7 ± 0.0
	10,000	—	—	1,281 ± 20	1.5 ± 0.1
PTI	0	50,650 ± 2,953	1.7 ± 0.2	1,379 ± 9	1.8 ± 0.1
	100	48,720 ± 1,019	1.7 ± 0.1	1,493 ± 4	1.7 ± 0.0
	1,000	47,527 ± 525	1.6 ± 0.0	1,491 ± 9	1.8 ± 0.1
	10,000	—	—	1,273 ± 13	1.7 ± 0.1

HM_w, high molecular weight; LM_w, low molecular weight.

shown in Figures 4 and 5. Second heating was attempted to erase the thermal history; however, the samples did not recrystallize so only the first scans were used to determine the transition temperatures. The neat PTM was an amorphous copolymer with a glass transition temperature (T_g) of ~58°C. It is well known that the molecular weight of polymer is a significant factor on T_g.[15] That is, a decrease in T_g can be related to a decrease in the molecular weight due to higher chain mobility. The T_g of PTM was found to trend upwards with degradation time as presented in Table II. This could be associated with the diffusion of low molecular weight PTM into water. Neat PTI is a semicrystalline polymer with a cold crystallization temperature of 159°C and a double melting temperature of 159°C and 214°C. Wang et al. reported a bimodal melting behavior of polyethylene produced by intercalated silicate with nickel diimine complex.[16] They also concluded that the polymers with low melting point and high molecular weight were firstly produced through a "chain walking" mechanism and followed by formation of polymer with high melting point and low molecular weight. PTI produced in this study by melt polycondensation did show a bimodal molecular weight of 1.4 kDa with 1.78 PDI and 50.7 kDa with 1.71 PDI. This bimodal molecular weight distribution can result in the bimodal melting behavior.

In addition, the cold crystallization temperature and melting temperatures of the PTI both increased as a function of the degradation time. The increase in the second melting peak position was more significant (an upward shift of 18°C) while the cold crystallization temperature only shifted by 3°C. The increase in the melting points can be attributed to the scission of the ester bonds in the polymer chain. The initial degradation in the amorphous phase could happen quickly since water attacks the weakly packed segments more easily. This resulted in increased chain mobility, and thus new, more organized crystalline regions occurred. As a result, this behavior called "cleavage-induced crystallization"[17–19] could increase the melting point of semi-crystalline PTI during the degradation.[20]

Since the melting enthalpy for 100% crystalline PTI was unknown, the degree of crystallinity (X_m) was not calculated. Therefore, the total melting enthalpies were used to monitor PTI's crystallinity. In general, the crystallinity of PTI tended to increase with the degradation. This could be explained by the behavior of semicrystalline polymers, such as PTI, undergoing partial degradation of the amorphous phase, as was previously described. Even though the crystallinity decreased gradually from 100 min until 10,000 min, it was still higher than that of neat PTI. In another study, Vasanthan and Gezer[21] investigated the crystallinity changes of as-cast PLLA films with degradation and concluded that a degradation of a restricted amorphous phase may cause an increase in crystallinity. Increased crystallinity induced by chain segmental motion may be a serious

Table II. Thermal Analysis Data of PTM and PTI Samples as a Function of Degradation Time

Polymer	Degradation Time (min)	$T_{5\%}$ (°C)	T_{max} (°C)	T_g (°C)	T_{cc} (°C)	T_{m1} (°C)	T_{m2} (°C)	ΔH_m (J/g)
PTM	0	201	—	−58	—	—	—	—
	10	197	—	−58	—	—	—	—
	100	187	—	−57	—	—	—	—
	1,000	192	—	−52	—	—	—	—
PTI	0	186	382	—	159	159	214	20.6
	100	208	384	—	160	161	228	28.0
	1,000	209	386	—	162	163	231	26.7
	10,000	223	386	—	162	163	232	25.6

T_g, glass transition temperature; T_{m1}, first melting temperature; T_{m2}, second melting temperature; T_{cc}, cold crystallization peak temperature; ΔH_m, melting enthalpy; $T_{5\%}$, temperature at 5% weight loss; T_{max}, temperature at 50% weight loss.

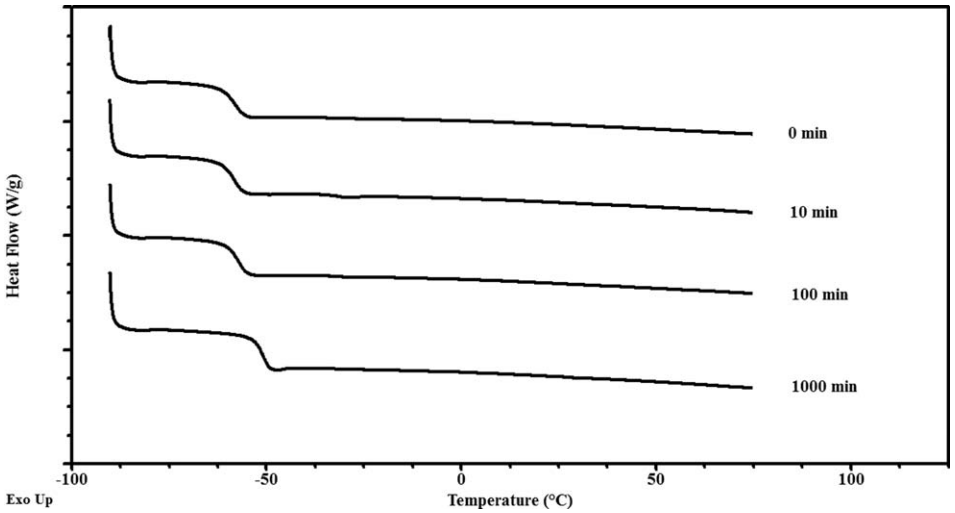

Figure 4. DSC thermograms of PTM after 0, 10, 100, and 1000 min of degradation showing transitions.

drawback for semicrystalline polymers used in biomedical implant applications because this recrystallinization can slow down the hydrolytic degradation of the material in the body.[22]

The thermal stability of the neat and degraded PTM and PTI samples was investigated by TGA. Table II presents these results including $T_{5\%}$ (5% weight loss) and T_{max} (50% weight loss) of the PTM and PTI samples. Neat PTM samples did not show 5 wt % loss until 201°C. Hydrolytic degradation reduced the thermal stability of amorphous PTM samples over time, as expected. Neat PTI thermal degradation temperatures $T_{5\%}$ and T_{max} were 186°C and 382°C, respectively. One would expect the thermal stability to eventually decrease as degradation proceeds. From the GPC study, it was suggested that the amorphous phase and small crystalline structures readily degraded or diffused out of PTI during the first 100 min, while the larger crystals did not experience degradation until 1000 min. This explains why the thermal stability of PTI samples shifted to higher temperatures with hydrolytic degradation. A similar thermal decomposition behavior for semicrystalline polymers was also reported by Olewnik et al.[20]

Nanomechanical Properties

The degraded PTM samples were gel-like and not suitable for full mechanical characterization. Therefore, in this study, mechanical property testing was performed on primarily the PTI samples as a function of the degradation time. Using AFM both qualitative and quantitative topography and nanomechanical information can be obtained. Figures 6–8 show height (topography), DMT modulus, and adhesion maps for neat PTI

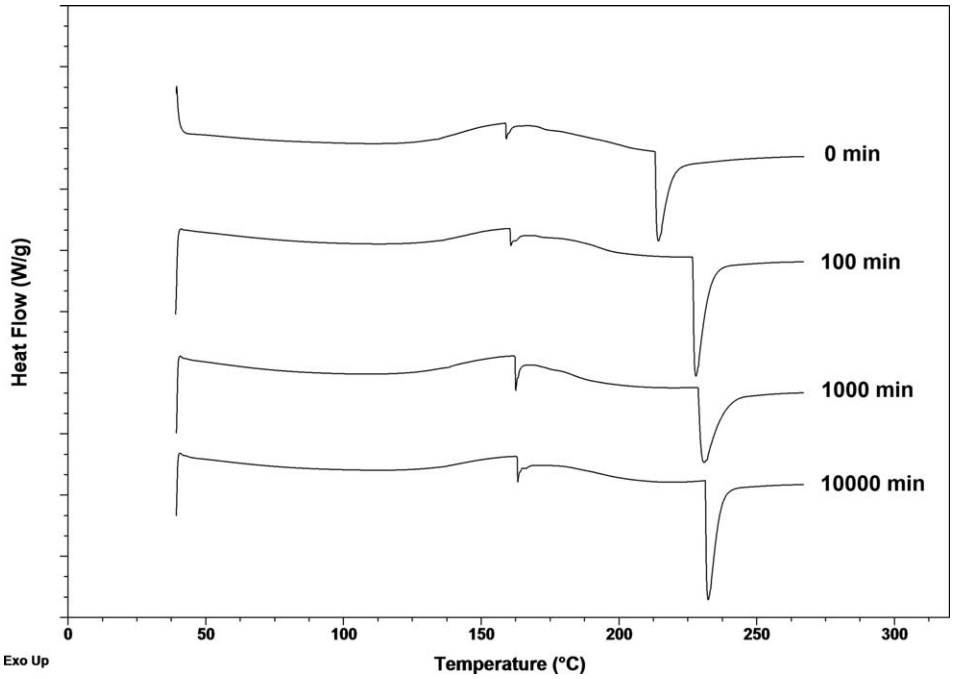

Figure 5. DSC thermograms of PTI after 0, 100, 1000, and 10,000 min of degradation showing phase transitions.

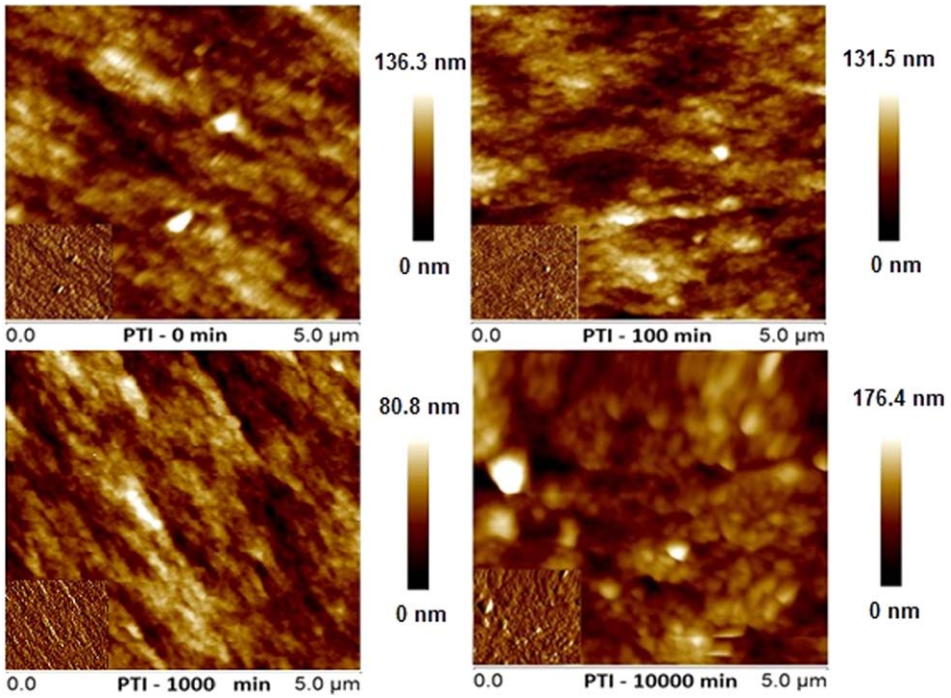

Figure 6. AFM topographical maps (5 × 5 μm^2) of neat PTI and PTI degraded for 100 min, 1000 min, and 10,000 min. The insets are peak force error images, which are the force signal error at each pixel location, and show rapid changes in surface morphology. [Color figure can be viewed in the online issue, which is available at wileyonlinelibrary.com.]

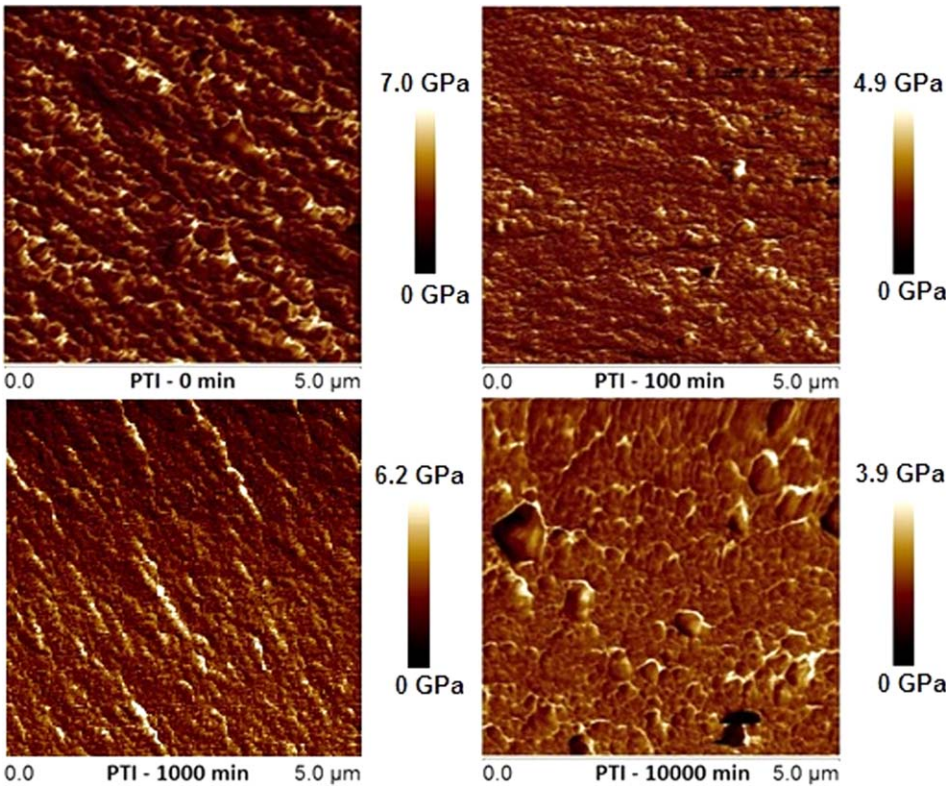

Figure 7. AFM DMT (Derjaguin-Muller-Toporov) modulus maps (5 × 5 μm^2) of neat PTI and PTI degraded for 100 min, 1000 min, and 10,000 min. [Color figure can be viewed in the online issue, which is available at wileyonlinelibrary.com.]

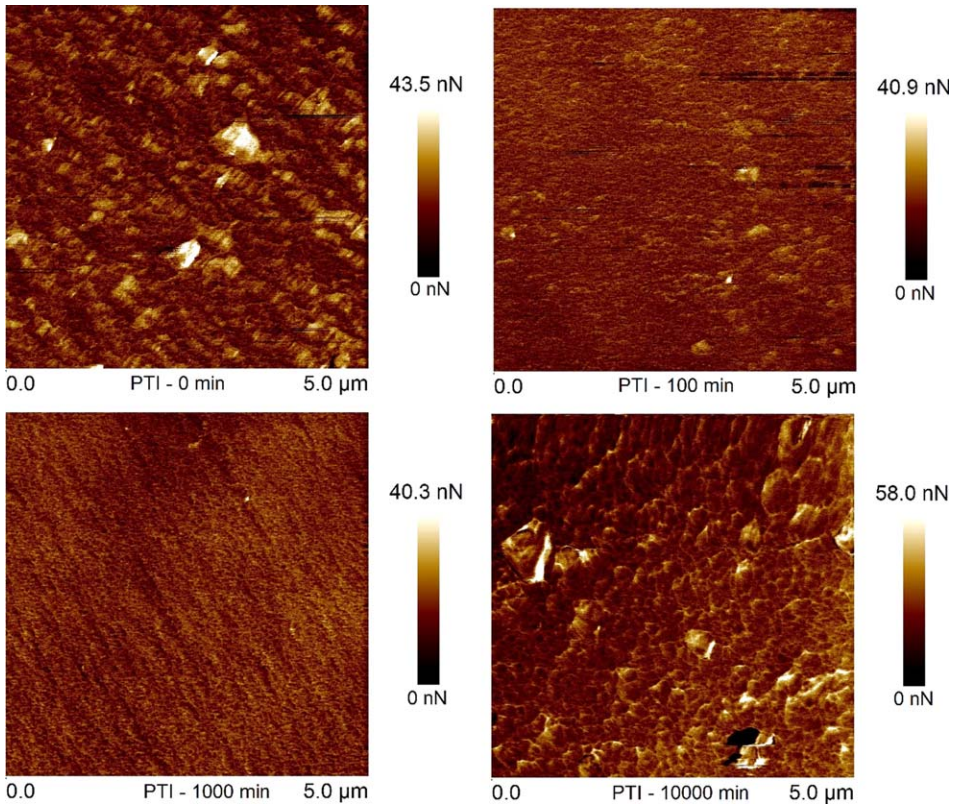

Figure 8. AFM adhesion maps ($5 \times 5\ \mu m^2$) of neat PTI and PTI degraded for 100 min, 1000 min, and 10,000 min. [Color figure can be viewed in the online issue, which is available at wileyonlinelibrary.com.]

and PTI samples degraded in DI water (pH 5.4) for different degradation times. Surface roughness of the samples increased with degradation time. The average AFM RMS roughness value for neat PTI was 16.17 ± 4.03 nm, and it did not increase significantly with degradation until 10,000 min. The average RMS roughness values for 100 and 1000 min degradation were 16.07 ± 3.65 nm and 10.63 ± 1.14 nm, respectively. At 10,000 min, the degraded PTI has an average roughness of 21.47 ± 4.11 nm. In addition to increased roughness, the degradation of PTI resulted in higher adhesion. The mean adhesion force increased from 23.67 ± 0.62 nN for neat PTI to 34.57 ± 2.55 n*N* for PTI degraded for 10,000 min.

The effect of hydrolytic degradation on the elastic modulus of PTI is shown in Figures 7 and 9. High modulus areas are visible in the PTI crystalline structure as the lighter colored areas while the darker colors are the low modulus, amorphous phase. According to the DMT modulus values, the neat PTI sample had an average surface modulus of 4.3 GPa. During hydrolytic degradation, the DMT modulus initially increased and then decreased significantly after 10,000 min of degradation time. Castilla-Cortázar et al. reported a similar trend; as degradation proceeded, Young's modulus of poly(ε-caprolactone) (PCL) networks increased at first and decreased slightly after week 38 of degradation in water and PBS.[23] After 10,000 min, the mean modulus of the degraded PTI sample was 1.8 GPa—a 58% decrease in modulus compared with the neat PTI sample. During the hydrolytic degradation, PTI demonstrated decreases in sample mass and molecular weight along with chemical changes such as the hydrolysis of backbone chain segments. These physical and chemical changes during degradation are significant factors in the loss of elastic modulus for the semicrystalline PTI bioplastic.[24,25]

In a single AFM experiment, PTM was found to be very soft with an elastic modulus of 7 MPa (Figure 10). The degraded PTM samples were gel-like and not suitable for AFM imaging.

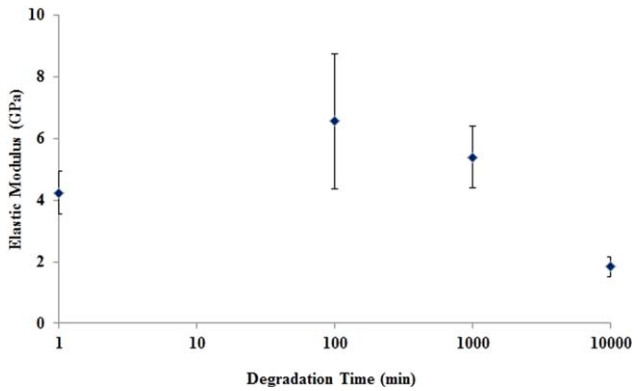

Figure 9. Elastic modulus of the neat and hydrolytically degraded PTI samples as a function of degradation time. [Color figure can be viewed in the online issue, which is available at wileyonlinelibrary.com.]

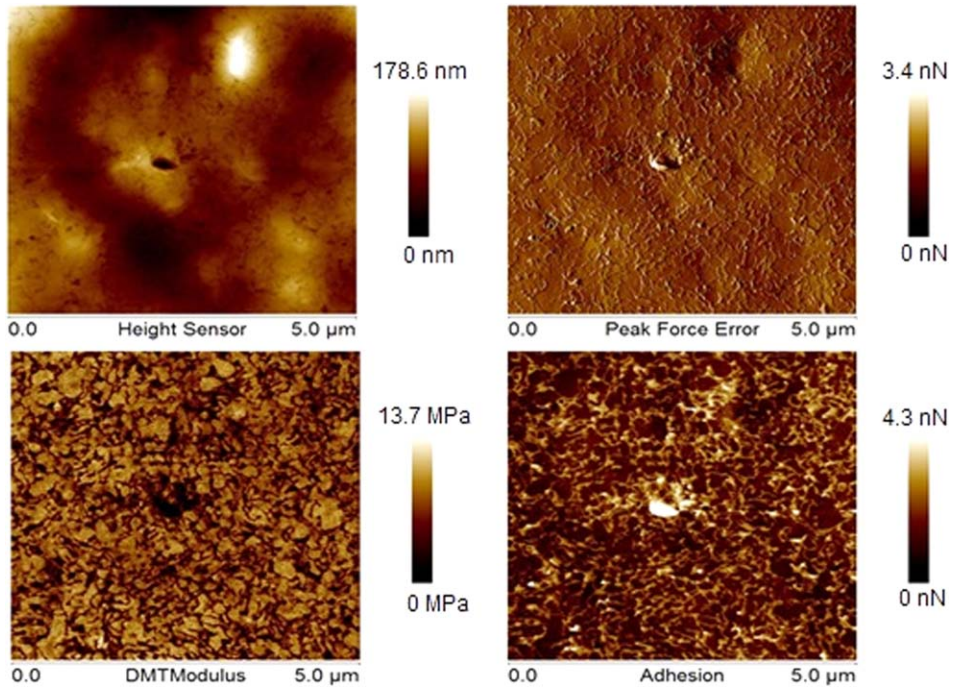

Figure 10. Neat PTM AFM maps (5 × 5 μm^2). [Color figure can be viewed in the online issue, which is available at wileyonlinelibrary.com.]

CONCLUSIONS

As part of efforts to develop degradable bioplastics, the hydrolytic degradation of PTM and PTI was performed in DI water (pH 5.4) at 25°C for up to 10,000 min in order to understand how mechanical properties are influenced by the degradation process. Significant degradation weight losses have been demonstrated for PTM and PTI with maximum values of 37 and 21 wt %, respectively, measured after one week. Results suggest that molecular weight was a key factor in not only the thermal properties but also surface mechanical properties of the bioplastics. The PTM samples had a soft and sticky nature—especially after degradation, uneven surface, and hygroscopic behavior. During hydrolytic degradation, the PTI samples showed major changes in their morphology, thermal properties, and surface mechanical properties after 1000 min. Degradation especially affected the amorphous region, leading to an increase in crystallinity. The changes in crystallinity showed a parallel behavior with the changes in elastic modulus. PTI with such an elastic modulus may be used for production of packaging material, disposable utensils, tableware, indoor furnishings, and more importantly, as a degradable biomaterial for biomedical applications. PTM could be used as a plasticizer for other degradable bioplastics, sensor applications, and drug delivery. Research with these polymers will continue with future polymer blends and all-green composite studies.

ACKNOWLEDGMENTS

A portion of this work was performed through the Sustainable Energy Research Center at Mississippi State University and supported by the US Department of Energy under award number DE-FG3606GO86025. The AFM, DSC, and TGA work were made possible through the National Science Foundation [CBET-0923474; CBET-0933493]. MSU's Bagley College of Engineering Ph.D. Fellowship and The Republic of Turkey's Ministry of National Education are also acknowledged for financial support.

REFERENCES

1. Williams, C. K.; Hillmyer, M. A. *Polym. Rev.* **2008**, *48*, 1.
2. Shikanov, A.; Kumar, N.; Domb, A. J. *Israel J Chem.* **2005**, *45*, 393.
3. Van Beilen, J. B.; Poirier, Y. *Plant J.* **2008**, *54*, 684.
4. Gandini, A. *Macromolecules* **2008**, *41*, 9491.
5. Philip, S.; Keshavarz, T.; Roy, I. *J. Chem. Technol. Biotechnol.* **2007**, *82*, 233.
6. Patel, M.; Narayan, R. Natural Fibers, Biopolymers, and Biocomposites; Boca Raton, FL: CRC Press Taylor and Francis Group; **2005**.
7. Ragauskas, A. J.; Williams, C. K.; Davison, B. H.; Britovsek, G.; Cairney, J.; Eckert, C. A.; Frederick, W. J.; Hallett, J. P.; Leak, D. J.; Liotta, C. L. *Science* **2006**, *311*, 484.
8. Okada, M. *Prog. Polym. Sci.* **2002**, *27*, 87.
9. Mohanty, A.; Misra, M.; Drzal, L. *J. Polym. Environment* **2002**, *10*, 19.
10. Willke, T.; Vorlop, K.-D. *Appl. Microbiol. Biotechnol.* **2004**, *66*, 131.
11. Vert, M. *Biomacromolecules* **2005**, *6*, 538.
12. Werpy, T.; Petersen, G.; Aden, A.; Bozell, J.; Holladay, J.; White, J.; Manheim, A.; Eliot, D.; Lasure, L.; Jones, S.; DTIC Document: **2004**.
13. Rowe, M. D.; Walters, K. B. *Annu. Tech. Conf. - Soc. Plast. Eng.* **2009**, *67th*, 508.

14. Pittenger, B.; Erina, N.; Su, C. *Application Note Veeco Instruments Inc* **2010**.
15. Avgoustakis, K.; Nixon, J. R. *Int. J. Pharmaceutics* **1991**, *70*, 77.
16. Wang, Q.; Liu, P. *J. Polym. Sci. Part A: Polym. Chem.* **2005**, *43*, 5506.
17. Fu, B. X.; Hsiao, B. S.; Chen, G.; Zhou, J.; Koyfman, I.; Jamiolkowski, D. D.; Dormier, E. *Polymer* **2002**, *43*, 5527.
18. Zong, X.-H.; Wang, Z.-G.; Hsiao, B. S.; Chu, B.; Zhou, J. J.; Jamiolkowski, D. D.; Muse, E.; Dormier, E. *Macromolecules* **1999**, *32*, 8107.
19. Fu, B. X.; Hsiao, B. S.; Chen, G.; Zhou, J.; Lin, S.; Yuan, J.; Koyfman, I.; Jamiolkowski, D. D.; Dormier, E. *Chinese J. Polym. Sci.* **2003**, *21*, 159.
20. Olewnik, E.; Czerwiński, W.; Nowaczyk, J. *Polym. Degrad. Stabil.* **2007**, *92*, 24.
21. Vasanthan, N.; Gezer, H. *J. Appl. Polym. Sci.* **2013**, *127*, 4395.
22. Auras, R. A.; Lim, L.-T.; Selke, S. E.; Tsuji, H. Poly (lactic acid): Synthesis, Structures, Properties, Processing, and Applications; Wiley: New York, **2011**.
23. Castilla-Cortázar, I.; Más-Estellés, J.; Meseguer-Dueñas, J.; Escobar Ivirico, J.; Marí, B.; Vidaurre, A. *Polym. Degrad. Stabil.* **2012**, *97*, 1241.
24. Sabino, M. A.; González, S.; Márquez, L.; Feijoo, J. L. *Polym. Degrad. Stabil.* **2000**, *69*, 209.
25. Sabino, M.; Sabater, L.; Ronca, G.; Müller, A. *Polym. Bull.* **2002**, *48*, 291.